ITC 2/52
Information Technology and Control
Vol. 52 / No. 2 / 2023
pp. 358-366
DOI 10.5755/j01.itc.52.2.32873

Brain Computer Interface Based on Motor Imagery for Mechanical Arm Grasp Control

Received 2022/11/28 | Accepted after revision 2022/03/06

HOW TO CITE: Shi, T. W., Chen, K.-J., Ren, L., Cui, W.-H. (2023). Brain Computer Interface Based on Motor Imagery for Mechanical Arm Grasp Control. *Information Technology and Control*, 52(2), 358-366. https://doi.org/10.5755/j01.itc.52.2.32873

Brain Computer Interface Based on Motor Imagery for Mechanical Arm Grasp Control

Tian-Wei Shi, Ke-Jin Chen
School of Computer Science and Software Engineering, University of Science and Technology Liaoning, 114051 Anshan, Liaoning, China

Ling Ren
School of Innovation and entrepreneurship, University of Science and Technology Liaoning, 114051, Anshan, China

Wen-Hua Cui
School of Computer Science and Software Engineering, University of Science and Technology Liaoning, 114051 Anshan, Liaoning, China

Corresponding author: tianweiabbcc@163.com

This paper puts forward a brain computer interface (BCI) system to realize the hand and wrist control using the Asea Brown Boveri (ABB) Mechanical Arm. This BCI system gathers four kinds of motor imaginary (MI) tasks (hand grasp, hand spread, wrist flexion and wrist extension) electroencephalogram (EEG) signals from 30 electrodes. It utilizes two fifth-order Butterworth Band-Pass Filter (BPF) with different bandwidths and normalization method to achieve the raw MI tasks EEG signals preprocessing. The main challenge of feature extraction is to analyze the MI task intention from the preprocessed EEG signals. Therefore, the proposed BCI system extracts eleven kinds of features in time domain and time-frequency domain and uses mutual information method to reduce the large dimension of the extracted features. In addition, the BCI system applies a single convolutional layer Convolutional neural networks (CNN) with 30 filters to implement the quaternary classification of MI tasks. Compared with existing research, the classification accuracy of this BCI system is increased by about 32%-35%. The actual mechanical arm grasping control experiments verifies that this BCI system has good adaptability.

KEYWORDS: Brain Computer Interface; Motor Imagery; Convolutional Neural Network; Quaternary Classification.

1. Introduction

Stroke is one of serious neurological injury that can disrupt blood supply to brain, leading to brain tasks injury, specifically motor deficit, such as loss of function in the arm, wrist or hands. The majority of patients with loss of upper limb motor function have amputations below the elbow [10]. The impulsive responses to motor tasks after stroke were found to be associated with activity feedback in the primary motor cortex and the quality of life (QoF) of stroke patients is affected as a result. Patients can improve their communication, daily life and exercise ability through some intelligent auxiliary methods or devices [2, 21].

Brain computer interface (BCI) systems gather electroencephalogram (EEG) signals to establish communication between spontaneous brain electrical activities and controlled devices [1]. They have been used in the rehabilitation field to help people with disabilities or motor deficit [8] including recovery of motor function of the upper limb [12] and stroke patients rehabilitation [3], etc. BCI system can be implemented in different ways, such as P300 [13], Steady-State Visual-Evoked Potential (SSVEP) [16] and Motor Imaginary (MI) [18], etc.

MI is one of the most studied types of EEG in the field of BCI. In fact, real movement, MI and somatosensory stimuli can regulate μ rhythm (8-13 Hz). MI and somatosensory stimuli can lead to the decay of Event Related Desychronization (ERD) and the increase of Event Related Synchronization (ERS). The most important fact for BCI is that the ERDs can be caused by MI in healthy people and intentional activity in disabled people. Since MI is independent of external stimuli, it has the higher potential for application. Grigorev et al. had realized vibrotactile neurofeedback training [7]. Wang et al. had used the multifractal detrended fluctuation analysis (MF-DFA) method to detect driver fatigue [20]. Palumbo et al. had provided state-of-the-art applications of wheelchair control and movement [17]. Shi et al. had utilized Common Spatial Pattern (CSP) and Convolutional Neural Network (CNN) to realized the low speed multi-rotor aircraft control [19]. Mwata-Velu et al. had employed Bidirectional Long Short-Term Memory (BiLSTM) network to carry out finger movements decoding [14]. Nann et al. had determined the link between BCI control performance over time and heart rate variability (HRV) and implemented assistive hand exoskeleton control [15], etc.

This proposed BCI system is constructed based on the EEG feature analysis of hand grasp, hand spread, wrist flexion and wrist extension MI tasks collected from 30 electrodes. Feature extraction is utilized to acquired the regular patterns of the brain activities and the effectiveness of feature extraction directly affects the final classification results. The Power Spectral Density (PSD) is unstable and sensitive to electrode position changes. The traditional Common Spatial Pattern (CSP) algorithm [9], and CSP-based algorithms are sensitive to noise [6, 5]. The Wavelet Transform (WT) is difficult to select suitable wavelet. To overcome these challenges, this BCI system utilizes eleven kinds of time and time-frequency domain hybrid features to classify MI tasks. Before feature extraction and classification, this BCI system utilizes a notch filter and two kinds of fifth-order Butterworth Band-Pass Filters (BPFs) with different bandwidths to eliminate the different frequencies noises and artifacts and applies normalization method to to eliminate the absolute amplitude and remain the relative amplitudes from the raw MI tasks EEG signals. The BCI system employs the mutual information method to reduce the dimension of the extracted features. Finally, it uses a single convolutional layer Convolutional Neural Networks (CNN) with 30 filters to implement MI tasks classification.

The rest of this study is organized as that: Methods are explained in Section 2. Sections 3 and Section 4 describe the actual mechanical arm control experiment results and discussions. Section 5 describes the conclusion.

2. Methods

2.1. Brain Computer Interface System

Figure 1 shows the overall structure of this proposed BCI system. The calibration experiment system is utilized to realize calibration training for subjects by simulating the actual hand and wrist movements. It is designed by Visual Studio 2019

Figure 1
Simplified BCI system structure

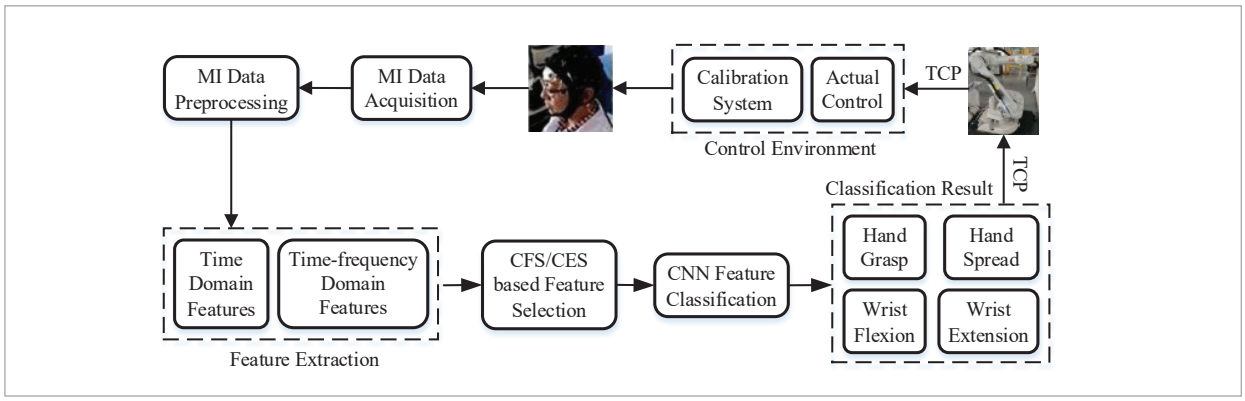

and OpenGL 4.6, and displayed on a 21-inch Liquid Crystal Display (LCD) monitor with the first person perspective. This BCI system is applied to realize grasping/spreading of objects and forward/backward movement of wrist for Asea Brown Boveri (ABB) mechanical arm using the hand grasp, hand spread, wrist flexion and wrist extension MI tasks respectively. The raw MI tasks EEG signals are recorded by 30 electrodes and preprocessed to eliminate the different frequencies noises and artifacts via two fifth-order BPFs with different bandwidths. The eleven kinds of features in time and time-frequency domain are extracted from the preprocessed EEG signals. After that, a forward stepwise searching feature selection strategy based on Correlation-based Feature Selection (CFS) and Classifier Subset Evaluation (CSE) is used to reduce the large dimension of the extracted features. A single convolutional layer CNN with 30 filters is adopts to implement the quaternary classification of MI tasks. The final classification output is converted into control command and sent to the mechanical arm via TCP.

2.2. MI Tasks Data Acquisition

Two males and four females, aged 21.4 ± 3.3 years (subjects 1-6), had participated in the calibration experiment. They sat comfortably in an armchair attaching with the Neuroscan (NuAmps) cap were closely attached to the scalp by 40 channels Ag/AgCl electrodes in accordance with the international 10-20 system. The linked ears electrodes were used as the reference

Figure 2
Timing schemes of acquisition the effective single MI task and continuous MI tasks EEG signals

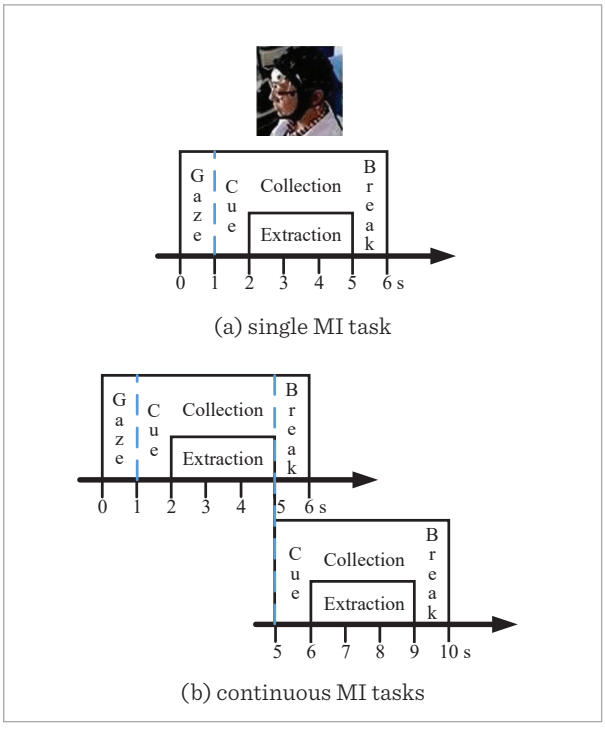

and the MI tasks were continuously recorded at 250 Hz with 22 bit from FP1, FP2, F7, F3, FZ, F4, F8, FT7, FC3, FCZ, FC4, FT8, T3, C3, CZ, C4, T4, TP7, CP3, CPZ, CP4, TP8, T5, P3, PZ, P4, T6, O1, OZ and O2 electrodes. They were told not to make any movements or sounds and looked at the 21-inch LCD screen for a

rest period of 3 min. This calibration experiment was run on the DELLXPS8940 with i7-11700 CPU, RTX 3060Ti graphics card and 32 GB RAM. It was consisted of MI tasks orderly training and random training. The subjects were required to complete each of the four MI tasks three times in each group of experiments with a total of 12 tasks. Each subject completed 10 groups on the same day and the interval between each group was 5 min. This study was approved by the Human Research Protections Program of University of Science and Technology Liaoning. Meanwhile, it was performed in accordance with the Declaration of Helsinki. All subjects were asked to read and sign an informed consent form before this study.

The timing schemes of acquisition the effective single MI task and continuous MI tasks EEG signals are shown in Figures 2(a) and 2(b), respectively. To remove the delay and signal instability, the single MI task was sampled in 2-5 s. Because MI task may be performed for a long time, it is necessary to divide the collected continuous MI task into multiple data segments.

2.3. MI Tasks Preprocessing

Before feature extraction, the collected MI tasks raw EEG signals need to eliminate the different frequencies noises and artifacts. Firstly, a notch filter was applied to get rid of the power-line interference at 50 Hz. Senondly, the fifth-order BPF in range of 1-100 Hz was utilized to remove the baseline drift and high frequency noises. Nextly, another fifth-order BPF in range of 8-30 Hz was also used to get the μ rhythm (8-13 Hz) and β rhythm (14-30 Hz) EEG signals. Then, the acquired EEG signals are normalized to eliminate the absolute amplitude and remain the relative amplitudes by using the Equation (1) [4].

$$z_i = \frac{w_i - \bar{w}}{\delta}. \tag{1}$$

where w_i is the input EEG signal, $\bar{w}$ is the mean of w_i, δ is the standard deviation of of w_i, z_i is the normalized EEG signal. Finally, EEG signals are segmented to extract epochs according to the timing schemes in Figure 2.

2.4. MI Tasks Feature Extraction

The main challenge of feature extraction is to extract enough representative features from MI tasks to classify them.

2.4.1. Time Domain Feature Extraction

In this step, five kinds of time domain features are extracted from the preproposed EEG signals. Define $y_j (1 \le j \le M)$ are samples in time domain, j is the index of current sample point, M is the number of samples, q is used to adjust the shape of probability distribution. The extracted time domain features can be described as that.

1 Root Mean Square

$$z_i = \frac{w_i - \bar{w}}{\delta}. \tag{2}$$

2 Renyi Entropy

$$Renyi = \log \frac{\sum_{j=1}^{M} {y_j}^2}{1-q}. \tag{3}$$

3 Hjorth Parameter

$$mobility = \sqrt{\frac{var(y_j')}{var(y_j)}}. \tag{4}$$

$$complexity = \frac{mobility(y_j')}{mobility(y_j)}. \tag{5}$$

4 Waveform Length

$$WL = \sum_j^M \left| y_j - y_{j-1} \right|. \tag{6}$$

5 Mean Absolute Value

$$\mu = \frac{1}{M} \sum_{j=1}^{M} \left| y_j \right|. \tag{7}$$

2.4.2. Time-frequency Domain Feature Extraction

In this step, two Higher-order Statistics (HOS) features are extracted from the preproposed EEG signals and four kinds of time-frequency domain features are extracted using the four levels of Wavelet Packet Decomposition (WPD). Define N is the length of each sub-band, $X\{x_1, x_2, ..., x_N\}$ and $Z\{z_1, z_2, ..., z_N\}$ are the two adjacent sub-bands after WPD.

1 Absolute Mean of Coefficients

$$\mu = \frac{1}{N} \sum_{i=1}^{N} \left| x_i \right|. \tag{8}$$

2 Average Power of Coefficients

$$P_{av} = \sqrt{\frac{1}{N} \sum_{i=1}^{N} x^2}. \tag{9}$$

3 Standard Deviation of the Coefficients

$$\sigma = \frac{1}{N}\sum_{i=1}^{N}(x_i - \mu)^2 . \quad (10)$$

4 Ratio of the Absolute Mean Values of Coefficients

$$\gamma = \frac{\frac{1}{N}\sum_{i=1}^{N}|x_i|}{\frac{1}{N}\sum_{i=1}^{N}|z_i|} . \quad (11)$$

5 Skewness of the Coefficients

$$S = \frac{1}{N}\sum_{i=1}^{N}\frac{(x_i-\mu)^3}{\sigma^3} . \quad (12)$$

6 Kurtosis of the Coefficients

$$K = \frac{1}{N}\sum_{i=1}^{N}\frac{(x_i-\mu)^{34}}{\sigma^{34}} . \quad (13)$$

2.5. MI Tasks Feature Selection

To reduce the large dimension of the extracted time domain and time-frequence domain features, the mutual information method was adopted. It is mainly used to measure the degree of nonlinear dependence between two random variables and closely related to the concept of entropy of a random variable. It can be describe as that:

$$I(X,Y) = H(X,Y) - H(X|Y) - H(Y|X), \quad (14)$$

where X and Y are the discrete arbitrary variables, $H(X|Y)$ and $H(Y|X)$ are the conditional entropies and $H(X, Y)$is the joint entropy of X and Y.

2.6. MI Tasks Classification

A single convolutional layer CNN with 30 filters includes the convolution layer, pooling layer, fully connected layer and activation functions was utilized to complete the quaternary classification. The extracted features were set as the input and the Rectified Linear Units (ReLU) was used as the activation function. After that, the pooling layer was adopted to reduce the feature dimension without changing the number of features and apply the max-pooling with pool size and step of 2. Final output features are converted to a one-dimensional array and fed into the fully connected layers. Meantime, the softmax activation function was applied in the output layer. The initial learning rate was set as 0.4. A total of 1440 trials are obtained in the calibration experiment, including 720 trials of orderly training and 720 trials of random training. In orderly training and random training, the 480 trials are used as training set and the other 240 trials are utilized as testing set respectively.

3. Actual Mechanical Arm Control Experiments

3.1. Experiment Setup

To verify the adaptability and control stability of this BCI system, twelve healthy subjects (subjects 1-6 had participated in the calibration experiment; three males and three females, aged 22.1 ± 4.2 years, had not participated in the calibration experiment (subjects 7-12)) were accomplished this experiment at the School of Innovation and entrepreneurship, University of Science and Technology Liaoning, Anshan, Liaoning, China. Subjects accomplishes the experiment on the same day.

The MI tasks preprocessing, MI tasks feature extraction, MI tasks feature selection and MI tasks classification algorithms were run on the DELLXPS8940 with i7-11700 CPU, RTX 3060Ti graphics card and 32 GB RAM. Before this experiment, subjects attached electrode caps and sat comfortably in an armchair to relax for 5 min.

3.2. Mechanical Arm Grasping Control

The subjects manually use the hand grasp and hand spread MI tasks to realize the grasping and spreading of objects and utilize the wrist flexion and wrist extension MI tasks to implement the forward and backward movement via the ABB mechanical arm. During this experiment, three object grasping positions in the vertical direction are separated by 30 cm from each other. The captured objects are green cube hard sponge block placed horizontally with the side length of 10 cm. The middle object grasping position is set as the initial position of the mechanical arm and the default height of the mechanical arm is 20 cm. The subjects perform the hand grasp MI task to lower the mechanical arm height. When the mechanical arm reaches the height of the object, it will automatically complete the grasping movement. On the contrary, the subjects perform the hand spread MI tasks to execute the spreading movement and control the mechanical arm return to the default height. The

Figure 3
Diagram of objects positions

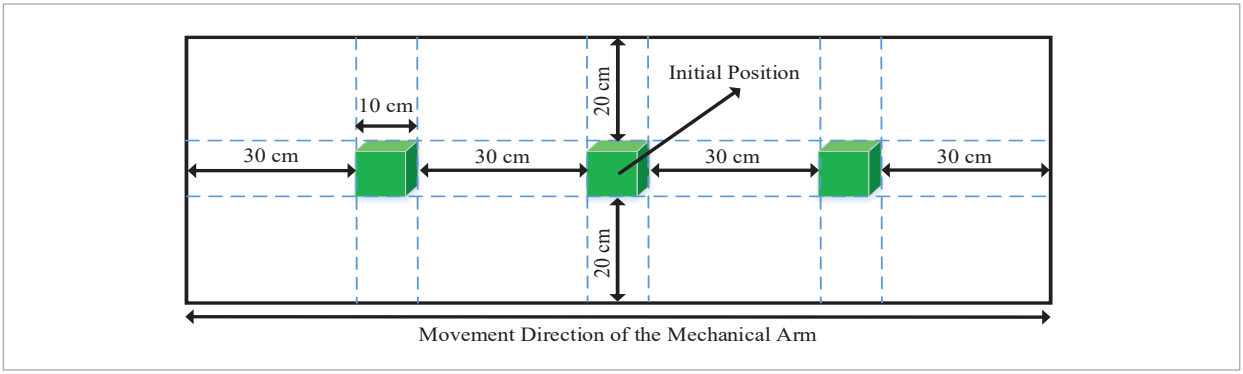

subjects are required to complete all three grasping tasks in any order. A bottom facing cameras is above the fingers of the mechanical arm and it transmits the real-time video by WIFI. The communication between the BCI system and the ABB mechanical arm is realized by TCP. Figure3 shows the objects positions. The black box is the experimental area and the dotted lines are the three object positions.

4. Results and Discussions

4.1. Results for MI Calibration Experiments

Figure 4 shows the classification accuracy (mean ± S.D.) of subjects 1-6. In orderly training (OT), the classification accuracies of subjects 1-6 are all higher than 86%. Subject 1 and subject 5 have the best classification accuracy of 91.67% and 90% respectively. In the random training (RT), as the subjects had gone through the previous orderly training, their classification accuracies are all higher than 88% and the classification accuracy of all subjects is increased by 0.97% on average. The classification accuracies of subject 4 and subject 6 are significantly improved by 1.67% and 1.66% respectively.

Figure 4
Classification accuracy of subjects 1-6 in orderly training and random training

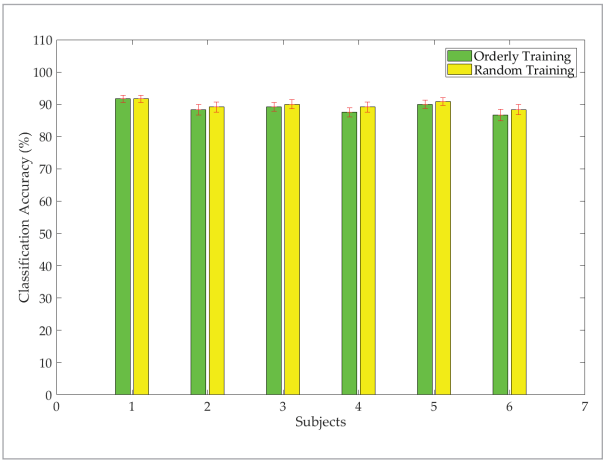

Compared with the traditional classification method (Time Domain Parameters and Shrinkage Regularized Linear Discriminant Analysis (TDP-SRLDA), Time/Time-frequency Domain and LSVM (TT-LSVM)) adopted by Lee et al. [10] and Attallah et al. [4], Table 1 shows that the CNN method (Ours) is used to achieve MI tasks classification and the classification accuracy is improved by about 32%-35%.

Table 1
Comparison of the classification accuracy (%)

Algorithm		1	2	3	4	5	6	Average
TDP-SRLDA	OT	55.67	55.33	56.67	57.95	58.17	56.67	56.74
	RT	56.17	55.67	57.17	58.17	58.33	57.67	57.2
TT-LSVM	OT	54.67	54.33	55.17	55.33	54.67	54.33	54.75
	RT	54.95	54.67	55.33	55.33	54.95	54.67	54.99
Ours	OT	91.67	88.33	89.17	87.5	90	86.67	88.89
	RT	91.67	89.17	90	89.17	90.83	88.33	89.86

4.2. Results for Actual Mechanical Arm Grasping Control Experiments

Table 2 shows the comparison of subjects 1-12 using this BCI system to implement the mechanical arm grasping control experiment (expected number of MI tasks (ENT), actual number of MI tasks (ANT), Time Cost (TC) and Classification Accuracy (CA)).

Table 2
Comparison results of subject 1-12 using the BCI system to complete the mechanical arm grasping control experiment

Subjects	ENT (N)	ANT (N)	TC (s)	CA (%)
1	40	43	199	93.02
2	40	44	208	90.91
3	40	44	214	90.91
4	40	44	218	90.91
5	40	43	204	93.02
6	40	44	224	90.91
7	40	48	335	83.33
8	40	47	294	85.11
9	40	47	302	85.11
10	40	49	324	81.63
11	40	49	342	81.63
12	40	46	279	86.97

To verify the good adaptability of this BCI system, the actual mechanical arm grasping control experiments is divided into two parts according to the time cost of subjects 7-12 in Table 2. Table 3 shows the time cost and classification accuracy comparison results of subjects 7-12 (ENT1/ENT2, ANT1/ANT2 and TC2/CA2 are the performance parameters of the first and second part respectively). Except for subject 7, subject 10 and subject 11, the classification accuracy of other subjects was higher than 80%. It is known that subject 7, subject 10 and subject 11 are unfamiliar with the MI tasks and have strong psychological cues to complete the experiments. This resulted in a lower classification accuracy. Compared with the first part, the difference ENT2/ANT2 is less than ENT1/ANT1. The classification accuracy of the second part is improved by about 6.18%-11.19%.

Table 3
Time cost and classification accuracy comparison results for subject 7-12

Subjects	ENT1 (N)	ANT1 (N)	ENT2 (N)	ANT2 (N)	CA1 (%)	CA2 (%)
7	17	22	23	26	77.27	88.46
8	17	21	23	26	80.95	88.46
9	18	22	22	25	81.82	88.00
10	17	22	23	27	77.27	85.19
11	17	22	23	27	77.27	85.19
12	18	22	22	24	81.82	91.67

5. Discussion

This paper proposed a novel BCI system to realize the mechanical hand and wrist control by using the four kinds of MI tasks e.g. hand grasp, hand spread, wrist flexion and wrist extension. In orderly training, the classification accuracies of all subjects are all higher than 86% and the subject 1 has the best classification accuracy of 91.67%. Since the subjects had gone through the previous orderly training, their classification accuracies are all higher than 88%. The classification accuracy of the subjects in random training is about 0.97% higher on average than the classification accuracy in orderly training. Compared with the traditional classification method adopted by Lee et al. [10] and Attallah et al. [4], the CNN method is used to achieve MI tasks classification and the classification accuracy is improved by about 32%-35%.

As shown in Table 2, subjects 7-12 need to perform more MI tasks to complete the actual mechanical arm grasping control experiments. The time cost of subjects 7-12 are about 1.25-1.71 times than subjects 1-6 and the classification accuracy is reduced by about 3.94%-11.39%. The subject 1 and subject 5 have the best experimental results. Subjects 1-6 have the better time cost and classification accuracy and have a good consistency between ENC and ANC. The command errors of subjects 1-6 are only 3-4, but subjects 7-12 are 6-9. This may be due to the following reasons: 1) they were not familiar with MI tasks and participated in the actual mechanical arm grasping control experiments directly; 2) performance of the MI task was affected by the strong psychological cues to complete the experiment.

Table 3 shows the two parts time cost and classification accuracy comparison results for subjects 7-12. The command errors of ENC1/ANC1 and ENC2/ANC2 are 4-5 and 2-4, respectively. The command errors are significantly reduced. On the contrary, since the subjects experienced the first part of the actual mechanical arm grasping control experiments, they obtained a more ideal classification accuracy in the second part. The classification accuracy is improved by about 7.92%-11.19%. The average classification accuracy of CA2 for subjects 7-12 is close to subjects 1-6. These verify that subjects can be familiar with the MI tasks and adapt to this BCI system in a short time.

Compared with the traditional classification method adopted by Lee et al. [10] and Attallah et al. [4], the CNN method is used to achieve MI tasks classification and the classification accuracy is improved by about 32%-35%.

6. Conclusion

This paper puts forward a brain computer interface (BCI) system to realize the grasp control using the ABB Mechanical Arm. This BCI system collects MI tasks EEG signals from 30 electrodes, e.g. hand grasp, hand spread, wrist flexion and wrist extension. It employs two fifth-order BPF with different bandwidths and normalization method to achieve the raw MI tasks EEG signals preprocessing. This proposed BCI system extracts MI tasks features in time domain and time-frequency domain and uses the mutual information method to reduce the large dimension of the extracted features. In addition, it utilizes a single convolutional layer CNN with 30 filters to implement the quaternary classification of MI tasks. Compared with early researches, the classification accuracy of this BCI system is increased by about 32%-35%. The actual mechanical arm grasping control experiments verifies that this BCI system has good adaptability.

In the future work, we will research the MI tasks of unilateral and bilateral upper limbs.

Acknowledgments

Tian-wei Shi has supported by the Natural Science Foundation project of Liaoning Province (2021-KF-12-06), Department of Education of Liaoning Province (2020FWDF01) and Project of Liaoning BaiQianWan Talents Program.

Wen-hua Cui has been supported by the National Natural Science Foundation of China (U1908218).

Conflict of interest

All authors declare that they have no conflict of interest.

Availability of data and material

Not applicable

Code availability

Not applicable.

Human and Animal Participants

This article contains the calibration experiments and actual mechanical arm control experiments with human participants. Five males and seven females participated in these experiments. This study was approved by the Human Research Protections Program of University of Science and Technology Liaoning. Simultaneously, it was performed in accordance with the Declaration of Helsinki. All participants were asked to read and sign an informed consent form before participating in the study.

References

1. Ahn, J. W., Ku, Y., Kim, D. Y., Sohn, J., Kim, J. H., Kim, H. C. Wearable in-the-Ear EEG System for Ssvep-based Brain-computer Interface. Electron Lett, 2018, 54(7), 413-414. https://doi.org/10.1049/el.2017.3970
2. Anitha, T., Shanthi, N., Sathiyasheelan, R., Emayavaramban, G., Rajendran, T. Brain-computer Interface for Persons with Motor Disabilities-A review. The Open Biomedical Engineering Journal, 2019, 13(1), 27-133. https://doi.org/10.2174/1874120701913010127
3. Al-Qazzaz, N. K., Alyasseri, Z. A. A., Abdulkareem, K. H., Ali, N. S., Al-Mhiqani, M. N., Guger, C. EEG Feature Fusion for Motor Imagery: A New Robust Framework Towards Stroke Patients Rehabilitation. Computers in Biology and Medicine, 2021, 137, 04799. https://doi.org/10.1016/j.compbiomed.2021.104799
4. Attallah, O., Abougharbia, J., Tamazin, M., Nasser, A. A. A BCI System Based on Motor Imagery for Assisting People with Motor Deficiencies in the Limbs. Brain Sci-

ences, 2020, 10(11), 864. https://doi.org/10.3390/brainsci10110864

5. Cherloo, M. N., Amiri, H. K., Daliri, M. R. Ensemble Regularized Common Spatio-Spectral Pattern (Ensemble RCSSP) Model for Motor Imagery-based EEG Signal Classification. Computers in Biology and Medicine, 2021, 135, 104546. https://doi.org/10.1016/j.compbiomed.2021.104546
6. Dong, E., Li, C., Li, L., Du, S., Belkacem, A. N., Chen, C. Classification of Multi-class Motor Imagery with a Novel Hierarchical SVM Algorithm for Brain-computer Interfaces. Medical and Biological Engineering and Computing, 2017, 55, 1809-1818. https://doi.org/10.1007/s11517-017-1611-4
7. Grigorev, N. A., Savosenkov, A. O., Lukoyanov, M. V., Udoratina, A., Shusharina, N. N., Kaplan, A. Y., Hramov, A. E., Kazantsev, V. B., Gordleeva, S. A BCI-Based Vibrotactile Neurofeedback Training Improves Motor Cortical Excitability During Motor Imagery. IEEE Transactions on Neural Systems and Rehabilitation Eegineering, 2021, 29, 1583-1592. https://doi.org/10.1109/TNSRE.2021.3102304
8. Jumphoo, T., Uthansakul, M., Uthansakul, P. Brainwave Classification Without the Help of Limb Movement and Any Stimulus for Character-writing Application. Cognitive Systems Research, 2019, 58, 375-386. https://doi.org/10.1016/j.cogsys.2019.09.002
9. Koles, Z. J. The Quantitative Extraction and Topographic Mapping of the Abnormal Components in the Clinical EEG. Electroencephalogr Clin Neurophysiol, 1991, 79(6), 440-447. https://doi.org/10.1016/0013-4694(91)90163-X
10. Lee, J. H., Oh, Y. E., Lee, H. J., Kim, K., Lee, S. J. Quantification of Upper Limb Isometric Force Control Abilities for Evaluating Upper Limb Functions Among Prosthetic Users. IEEE Transactions on Neural Systems and Rehabilitation Engineering, 2021, 29, 2559-2568. https://doi.org/10.1109/TNSRE.2021.3133539
11. Lee, S. B., Kim, H. J., Kim, H., Jeong, J. H., Lee, S. W., Kim, D. J. Comparative Analysis of Features Extracted from EEG Spatial, Spectral and Temporal Domains for Binary and Multiclass Motor Imagery Classification. Information Sciences, 2019, 502, 199-200. https://doi.org/10.1016/j.ins.2019.06.008
12. Machado, T. C., Carregosa, A. A., Santos, M. S., Ribeiro, N. M. D., Melo, A. Efficacy of Motor Imagery Additional to Motor-Based Therapy in the Recovery of Motor Function of the Upper Limb in Post-Stroke Individuals: A Systematic Review. Topics in Stroke Rehabilitation, 2019, 26(7), 548-553. https://doi.org/10.1080/10749357.2019.1627716
13. Mudabbir, M. A. M., Mundlamuri, R. C., Aravind, K. R., Narayanan, M., Alladi, S., Shivashankar, N., Kenchaiah, R., Asranna, A., Viswanathan, L. G., Bhargava, G. K., Velmurugan, J., Thennarasu, K., Rajan, J., Kulanthaivelu, K., Bharath, R. D., Saini, J., Sinha, S. EEG-based P300 in Mesial Temporal Lobe Epilepsy and its Correlation with Cognitive Functions: A Case-Control Study. Epilepsy and Behavior, 2021, 123, 108279. https://doi.org/10.1016/j.yebeh.2021.108279
14. Mwata-Velu, T., Avina-Cervantes, J. G., Cruz-Duarte, J. M., Rostro-Gonzalez, H., Ruiz-Pinales, J. Imaginary Finger Movements Decoding Using Empirical Mode Decomposition and a Stacked BiLSTM Architecture. Mathematics, 2021, 9(24), 3297. https://doi.org/10.3390/math9243297
15. Nann, M., Haslacher, D., Colucci, A., Eskofier, B., von Tscharner, V., Soekadar, S. R. Heart Rate Variability Predicts Decline in Sensorimotor Rhythm Control. Journal of Neural Engineering, 2021, 18(4), 0460b5. https://doi.org/10.1088/1741-2552/ac1177
16. Ojha, M. K., Mukul, M. K. A Novel Approach Based on EMD to Improve the Performance of SSVEP Based BCI System. Wireless Personal Communications, 2021, 118(4), 2455-2467. https://doi.org/10.1007/s11277-021-08135-6
17. Palumbo, A., Gramigna, V., Calabrese, B., Ielpo, N. Motor-Imagery EEG-Based BCIs in Wheelchair Movement and Control: A Systematic Literature Review. Sensors, 2021, 21(18), 6285. https://doi.org/10.3390/s21186285
18. Pillette, L., Roc, A., N'Kaoua, B., Lotte, F. Experimenters' Influence on Mental-Imagery based Brain-Computer Interface User Training. International Journal of Human-Computers Studies, 2021, 149, 102603. https://doi.org/10.1016/j.ijhcs.2021.102603
19. Shi, T. W., Chang, G. M., Qiang, J. F., Ren, L., Cui, W. H. Brain Computer Interface System Based on Monocular Vision and Motor Imagery for UAV Indoor Space Target Searching. Biomedical Signal Processing and Control, 2023, 79, 11199-104114. https://doi.org/10.1016/j.bspc.2022.104114
20. Wang, F., Wang, H., Zhou, X., Fu, R. A Driving Fatigue Feature Detection Method Based on Multifractal Theory. IEEE Sensors Journal, 2022, 22(19), 19046-19059. https://doi.org/10.1109/JSEN.2022.3201015
21. Zabcikova, M., Koudelkova, Z., Jasek, R., Navarro, J. Recent Advances and Current Trends in Brain-Computer Interface Research and their Applications. International Journal of Developmental Neuroscience, 2022, 82(2), 107-123. https://doi.org/10.1002/jdn.10166